

# Relationship between size and translational velocity of bubbles driven by acoustic radiation force

音響放射力で駆動される気泡の移動速度と気泡サイズの関係性

Kenji Yoshida<sup>1†</sup>, Masaaki Omura<sup>1,2</sup>, Shinnosuke Hirata<sup>1</sup> and Tadashi Yamaguchi<sup>1</sup>  
(<sup>1</sup>Center for Frontier Medical Engineering, Chiba Univ.; <sup>2</sup>Fac. Eng., Univ. Toyama  
吉田憲司<sup>1†</sup>, 大村眞朗<sup>1,2</sup>, 平田慎之介<sup>1</sup>, 山口匡<sup>1</sup> (<sup>1</sup>千葉大・CFME, <sup>2</sup>富山大・工)

## 1. Introduction

Acoustic radiation force has been applied for non-contact manipulation and levitation of microscopic objects. It has often been used for controlling the behaviors of bubbles as contrast agents in contrast-enhanced ultrasonography. We have proposed the method for distinguishing the lymph channels from surrounding tissue, where bubble translation caused by the acoustic radiation force was quantitatively evaluated by the Doppler method. Since the acoustic radiation force acting on bubbles significantly depends on the relationship between bubble size and incident ultrasound frequency, i.e. resonance condition, the size bubble size probably affects the quality of the image obtained by the proposed method. Therefore, we investigated the translation of bubbles with different size distributions. In this paper, we reported the translational velocity depending on the bubble size.

## 2. Materials and Methods

Laboratory-made bubbles were composed of lipid shell and vaporized perfluorohexane (C<sub>6</sub>F<sub>14</sub>) as internal gas. First, 22.77 mg of hydrogenated soybean phosphatidylcholine (HSPC) was dispersed into 10 mL of phosphate buffered saline. Then DSPE-PEG2000 (10 mg) were added to the dispersion. The resultant lipid dispersion and the C<sub>6</sub>F<sub>14</sub> were manually mixed with a volume ratio of 2:1 by two syringes. This process was defined as the first mixing. When fabricating bubbles with a mean radius larger than approximately 5 μm, the bubble size distribution was controlled by their buoyance after the first mixing. The bubble suspension was poured in a buret, and 2 mL of the bubble suspension, including bubbles with smaller radii, were collected after a specific time. When fabricating bubbles with smaller radii, we added the second mixing process using an ultrasonic homogenizer. This process contributed to making smaller bubbles by the destruction of larger bubbles. After the second mixing, smaller bubbles in the suspension were

collected by the same method as above. The size distribution and number density of the bubbles were quantified by using a hemocytometer before ultrasound examinations.

The bubble suspension of approximately 0.02 mL was sent a flow channel formed in a gel phantom. To make the static situation like lymph channel, i.e. almost no or slow flow condition, we waited for 30 s after sending the suspension. Then the ultrasound emitting and receiving was repeated using a single element concave transducer with F-number of 2 and the center frequency of 10 MHz, which was located approximately 19 - 20 mm above the channel. The ultrasound beam was focused towards the upper surface of the channel using a precise positioning stage. The point spread functions (PSF) in the lateral and depth direction at the focus were approximately 0.32 mm and 0.09 mm, respectively. The ultrasound pulse was repeatedly emitted and received with a pulse repetition frequency of 5 kHz for a duration of 0.4 s. The echo signal was digitized with a sampling frequency of 500 MHz and a quantization rate of 12 bits using an oscilloscope. The conditions for negative peak sound pressure of incident ultrasound were 1.2 MPa; the corresponding mechanical index was 0.32.

The echo intensity and translational velocity of bubbles were analyzed by the Doppler method as shown in Ref. 1. The spectrum of Doppler signal (signal in the direction of pulse repetition time) at the specific depth was analyzed. The translational velocity of bubbles ( $v_{\text{travel}}$ ) was calculated from the expected value of the normalized spectrum using the following expression,

$$v_{\text{travel}} = \frac{\Delta f}{2f_0 + \Delta f} c, \quad (1)$$

where  $f_0$ ,  $\Delta f$  and  $c$  were the center frequency of incident ultrasound, the expected value of normalized spectrum, and the speed of sound of the surrounding phantom. The echo powers from a stationary object and moving one were defined as the value of the Doppler spectrum at  $f = 0$  and the integrated value of the spectrum except for  $f = 0$ , respectively. The integrate frequency range was from -1.25 kHz to 1.25 kHz. In this report, the former and

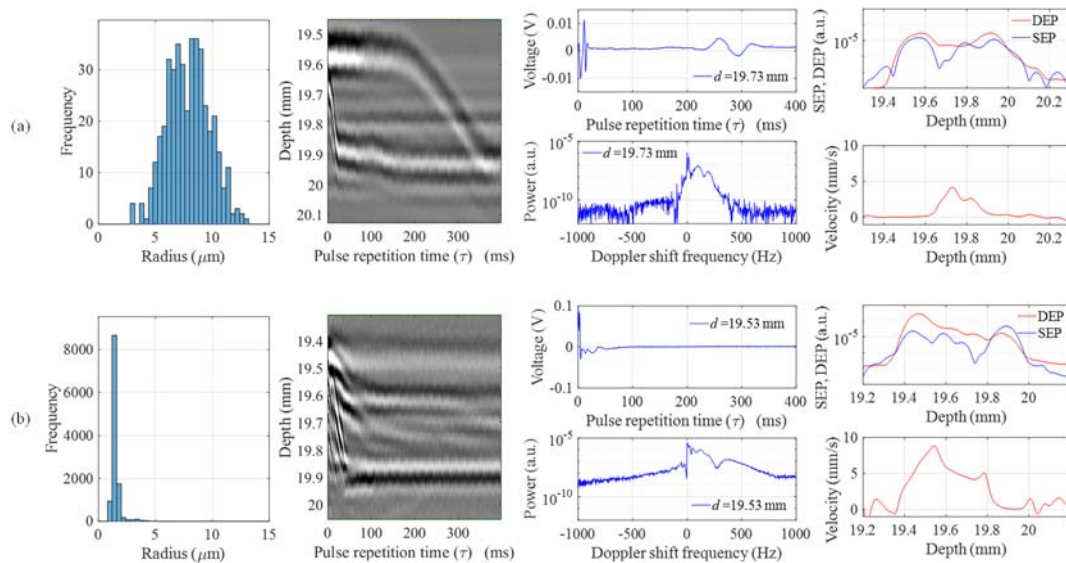


Fig. 1 Analyzed data in two cases for bubbles with different size distribution. Left column: distributions of bubble radius, Second left column: M-mode images, third left column: Doppler signal (upper) and Doppler spectrum (lower) at a specific depth, right column: changes of SEP and DEP (upper), and translational velocity (lower) in the depth direction. Radius (mean  $\pm$  standard deviation) and the number density of bubbles in the suspension were (a)  $7.91 \pm 1.87 \mu\text{m}$  and  $1.97 \times 10^{11} \text{ 1/m}^3$  and (b)  $1.49 \pm 0.39 \mu\text{m}$  and  $8.92 \times 10^{12} \text{ 1/m}^3$ .

latter were denoted as stationary echo power (SEP) and dynamic echo power (DEP), respectively.

### 3. Results

**Figure 1** shows examples of distribution of bubble radius and corresponding analyzed data in two cases. In the case of (a), echoes from bubbles moving away from the transducer were observed at  $0 \text{ s} < \tau < 20 \text{ ms}$  and  $250 \text{ ms} < \tau < 350 \text{ ms}$  in the M-mode image. The slower translation was typically observed in the condition for this size distribution. However, the more rapid translation just after the start of ultrasound exposure, such as those at  $0 \text{ s} < \tau < 20 \text{ ms}$  was occasional. Doppler spectrum had two peaks corresponding to the slow and rapid translations at  $\Delta f > 0$ . SEP was approximately equal to DEP around upper and lower channel walls, resulting in the small translational velocity. In the case of (b), the M-mode image suggested that almost all bubbles moved away from the transducer at  $\tau < 50 \text{ ms}$ . The rapid decrease of Doppler signal leading to broadband noise in the Doppler shift spectrum suggested many bubbles were collapsed. Unlike the case of (a), DEP was much larger than SEP except for the lower channel wall. The translational velocity of bubbles was higher than those in (a) in the wide depth range.

The average of the translational velocity of bubbles in the channel was measured in several conditions for bubble size distribution. **Figure 2** shows the average translational velocity versus bubble radius, where vertical error bars were standard deviation of the average translational

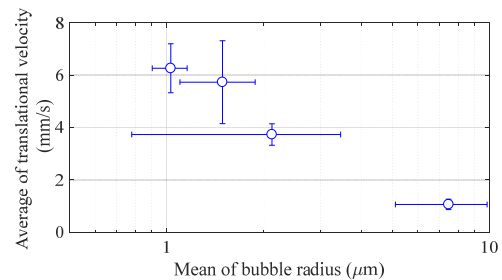


Fig. 2 Relationship between the mean of bubble radius and translational velocity.

velocity ( $n = 10$ ) and horizontal ones were standard deviation of bubble radius calculated from the distribution, respectively. The translational velocity of bubbles increased with decreasing in the mean of bubble radius in the range of  $1 - 10 \mu\text{m}$ .

### 4. Conclusions

This report investigated bubble translation induced by acoustic radiation force. In the case of bubbles with the mean radius of  $1 - 10 \mu\text{m}$  under the exposure of ultrasound with 10-MHz center frequency, it was found that the translational velocity increased with decreasing in the mean bubble.

### Acknowledgment

This work was partly supported by JSPS Core-to-Core Program JPJSCCA20170004 and JSPS Grant-in-Aid for Scientific Research 19H04436, and Institute for Global Prominent Research at Chiba University.

### References

1.K. Yoshida et al.: Jpn. J. Appl. Phys. **59** (2020) SKKE07.